

Effects of Flame Instabilities in Hydrogen-Air Explosions

Woogyung Kim¹, Tomomi Imamura², Toshio Mogi², Ritsu Dobashi²

¹Hiroshima University,

Higashi-Hiroshima, Hiroshima, Japan

²The University of Tokyo

Hongo, Tokyo, Japan

1 Introduction

A wrinkled flame has a larger surface area than a smoothly propagating flame and results in acceleration of flame propagation. Since the intensity of blast wave depends on the flame propagation and such acceleration might cause the strong blast wave lead to the considerable damages, the accelerative dynamics are important parameters for an appropriate risk assessment of accidental gas explosions [1]. It is known that the flame wrinkling is spontaneously generated by flame front instabilities such as diffusional-thermal and hydrodynamic instabilities although the gas is initially in homogeneous mixing conditions. The transition to cellularity in expanding spherical flames has been studied in recent years [2-8]. However, although the flame acceleration for the onset of instability studied by a number of theoretical and experimental studies, the further studies on this issue is needed for the appropriate risk assessment against to accidental hydrogen explosions. In view of above consideration, the purpose of this study is to investigate the effects of flame instabilities on spherically propagating of hydrogen-air flames. The first objective of the present study, the cell evolutions due to diffusional-thermal and hydrodynamic instabilities of hydrogen-air flames are investigated analytically and experimentally. The additional objectives of the study are the evaluations of critical points represented as the critical Peclet numbers, $Pe_c = r_c/\delta$, which is the critical flame radius, r_c , scaled by the flame thickness, δ , for the onset of flame instability and the effects of flame instabilities on the acceleration of flame speed.

2 Experimental set-up

In the present study, the experiments were performed in a spherical bubble with hydrogen-air mixtures and in a spherical combustion chamber with an inner diameter of 0.70 m to observe the developments of wrinkling on the flame surface. For the soap bubble experiment, the experimental apparatus consisted of a gas supplying system with designed bubble apparatus, an ignition system, the high-speed Schlieren photography system. A more details of the apparatus design and the experimental procedure is given in [1]. The flame images were photographed by using a high speed camera at 5000 frames per second.

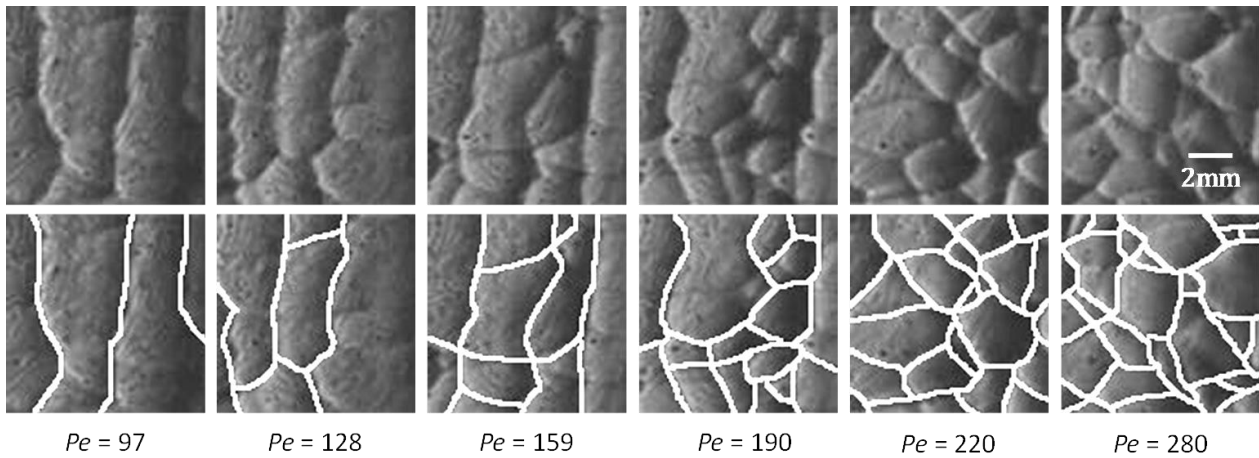


Figure 1. Images of cellular formation of hydrogen-air flame, $\phi = 0.8$ at 0.1MPa

To investigate the effects of flame front instabilities in particular hydrodynamic instability on the cellular flame surface, the large volume vessel comprised of quartz glass windows of 150 mm on the sidewalls of the chamber is manufactured. The total volume of the chamber was 180 L. The propagating flame of hydrogen-air mixtures was imaged with shadow photography and recorded by using the high speed camera at 3000 frames per second. The hydrogen and air were supplied by their individual partial pressures and a sample was taken from the top and bottom of the chamber by using a concentration meter. The mixture was ignited by an electric spark at the center of the chamber. These experiments were conducted in quiescent conditions at initial pressures ranging from 0.05 MPa to 0.20 MPa.

3 Results and discussion

Figure 1 shows the Schlieren image observation of the developments of cells on the surface of hydrogen-air flame of $\phi = 0.8$ at 0.1 MPa. The images of cellular formations of hydrogen-air flame are analyzed by using image thresholding technique which isolates the objects by converting grayscale images into binary images. In the present study, the part of flame image is focused for analyzing images. The thresholding images of cellular formation of hydrogen-air flame, $\phi = 0.8$ at 0.1 MPa are shown in Fig.1. The cell boundary on the threshold images is shown by the white line, which indicates the cell developments. The onset of cracks on the surface is formed by the electrodes and the large cracks formed start to branch along the realms of high curvature with increasing values of the Peclet number, $Pe = r/\delta$, where $\delta = (\lambda/c_p)/(\rho/S_L)$. The cells are created by expanding existing cells and it propagates across the surface. Consequently, such flame becomes fully cellular by diffusional-thermal and hydrodynamic instabilities.

The images of the evolution of cellular structure revealed by hydrogen-air flame with Peclet number, $\phi = 0.8$ at 0.1 MPa, $\phi = 5.0$ at 0.15 MPa and measured cell size with Pe are shown in Fig.2. The wrinkling for hydrogen air flame of $\phi = 0.8$ at 0.1 MPa must be caused by the effect of diffusional-thermal instability. It is reasonable to suggest that the influence of the mass diffusivity strongly dominated, the thermal diffusivity weakly affected, consequently a cellular shape observed. For hydrogen air flame of $\phi = 5.0$ at 0.15 MPa, although the value of Le for rich hydrogen flame no less than the unity, the flame is cellularly wrinkled, because the formations of cellular structure are affected intensively by the hydrodynamic instability as the initial pressure increases. The measured cell size for a $Le < 1$ flame decreases with Pe and

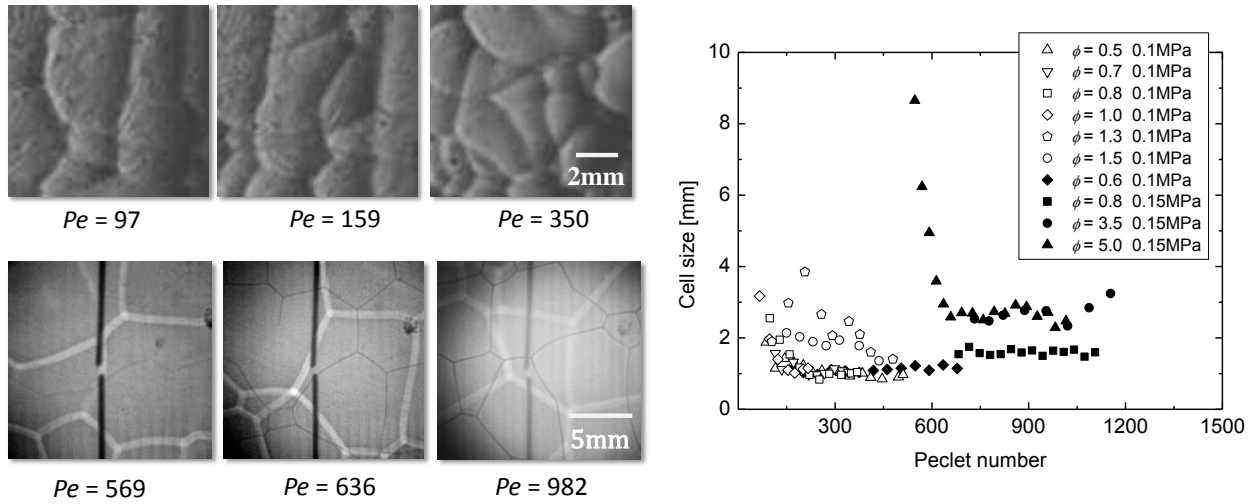


Figure 2. Evolution of cellular structure revealed by hydrogen-air flame with Peclet number, $\phi = 0.8$ at 0.1 MPa, $\phi = 5.0$ at 0.15 MPa and measured cell size with Peclet number.

it becomes constant. The values of cell size at high initial pressure are greater than that of at 0.1 MPa. In addition, the observed cell on the surface demonstrates the size of cells formed by hydrodynamic instability is greater than that of cells generated by diffusional-thermal instability, because the formed cells due to hydrodynamic instability are finally developed as large cusp. This result also reported in experimental results [4, 6].

The critical flame radius, r_c , and critical Peclet number, Pe_c , associated with onset of instability for hydrogen-air mixtures at different initial pressure respectively are shown in Fig. 3. It is first seen that the increasing trend of r_c with the concentration and decreasing tendency with the increasing in the initial pressure. The increasing results of r_c with increasing ϕ indicate that the flame is cellularly stable contribute to flame stability. In other words, the flame become cellularly unstable with decreasing ϕ , because of the increasing in the intensity of diffusional-thermal instability corresponded to decrease of Lewis number, Le . The decreasing results of r_c with increasing P_0 demonstrate that the flame becomes thinner and the hydrodynamic instability dominates the propagation dynamics causing the flame to cellular because the flame thickness decreases with increasing P_0 in Fig.3. The values of Pe_c also increase with increasing ϕ due to the stabilization, which leads to weaker cellular developments on the surface. In the range of $\phi = 0.5$ -2.0, the values of Pe_c increase with P_0 because of decreasing the flame thickness. This result demonstrates that the hydrodynamic instability is promoted with increasing with P_0 .

Such onset of the cell on the structure of the expanding spherical hydrogen-air flame due to diffusional-thermal and hydrodynamic instabilities cause the increase of the flame speed. The laminar burning velocity, $S_l = S_0 (T_u/T_{u0})^\alpha (P/P_0)^\beta$, without the wrinkling on the flame surface can be calculated when T_u is the unburned gas temperature defined as $T_u = T_{u0} (P/P_0)^{\gamma-1/\gamma}$, α and β are the characteristic constants related to the fuel and concentration. The ratio of increase in the burning velocity, S_m/S_l , where S_m is measured burning velocity, which defined as $S_m = (dr/dt)/\varepsilon$ with ϕ at different initial pressures also is shown in Fig.3. The ratio of increase in the burning velocity decreases with ϕ . It is reasonable to explain that this is the flame is unstable due to the intensity of diffusional-thermal instability and lead to the

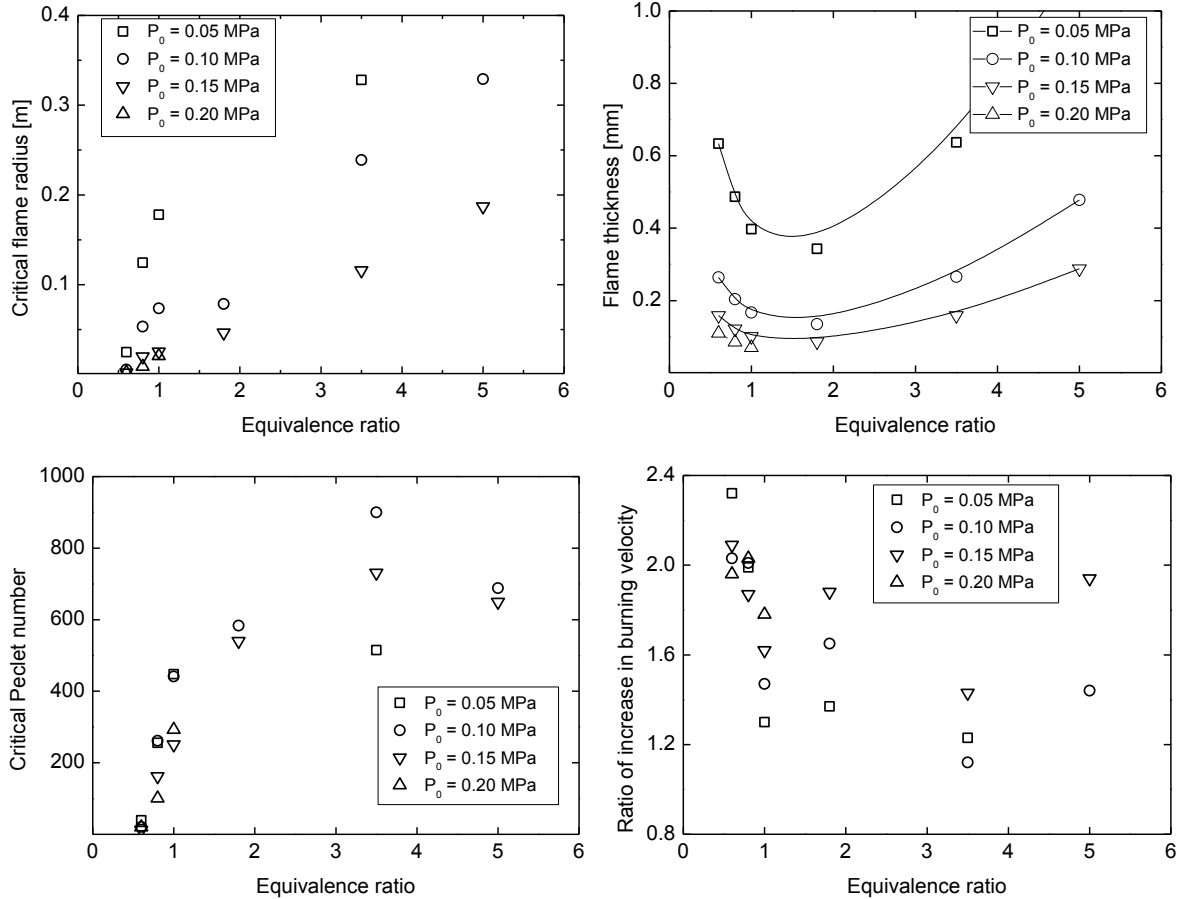


Figure 3. Experimental critical flame radius, flame thickness, critical Peclet number ratio of increase in burning velocity for hydrogen in air at different initial pressures versus equivalence ratio.

increasing in the flame speed. The second tendency is that the ratio of increase in the burning velocity increase with increasing with P_0 . Such results of the increasing trend by increasing with P_0 the indicate that the thin flame by increasing with P_0 becomes unstable due to the hydrodynamic instability.

4 Conclusions

Experiments have been conducted to examine the flame instabilities on expanding spherical propagation of hydrogen-air flames. The cell formation and development on the surface of hydrogen-air flame were investigated as a function of Pe using image thresholding technique. The cells began to start along the realms of high curvature and propagated across the surface with increasing Pe . The cell size of the flames wrinkled due to diffusional-thermal and hydrodynamic instabilities are measured. It is shown the values of cell size by hydrodynamic instability are greater than that of cells generated by diffusional-thermal instability. The critical flame radius, r_c , and critical Peclet number, Pe_c , for the onset of instability are characterized. The values of Pe_c increased with increasing ϕ by the stabilization and increase with P_0 by decreasing the flame thickness. Such results Pe_c is promoted by diffusional-thermal as well as

hydrodynamic instabilities. In the present study, the effects of the instabilities on the flame speed are estimated comparing the ratio of increase in the burning velocity. The ratio of increase in the burning velocity decreased with ϕ and increased with P_0 . Our results demonstrate that the cellular flame due to the flame instabilities might cause the increase in the flame speed and thereby lead to the strong blast wave lead to considerable damages generates. Further investigations with thinner flames at initial high pressure or large scale are needed to develop this issue experimentally and theoretically.

References

- [1] Kim WK, Mogi T, Dobashi R, (2014) Effect of propagation behaviour of expanding spherical flames on the blast wave generated during unconfined gas explosions. *Fuel*. 128: 396-403.
- [2] Bechtold JK, Matalon M. (1987) Hydrodynamic and diffusion effects on the stability of spherically expanding flames. *Combust. Flame* 67: 77–90.
- [3] Bradley D. (1999) Instabilities and flame speeds in large-scale premixed gaseous explosions. *Phil. Trans. R. Soc. Lond. A* 357: 3567–3581.
- [4] Bradley D, Harper CM. (1994) The development of instabilities in laminar explosion flames. *Combust. Flame* 99: 562–572.
- [5] Wu F, Jomass G, Law CK. (2013) An experimental investigation on self-acceleration of cellular spherical flames. *Proc. Combust. Inst.* 34: 937–945.
- [6] Kim WK, Mogi T, Kuwana K, Dobashi R, (2015) Self-similar propagation of expanding spherical flames in large scale gas explosions. *Proc. Combust. Inst.* 29: 1527–1535.
- [7] Addabbo R, Bechtold JK, Matalon M. (2002) Wrinkling of spherically expanding flames. *Proc. Combust. Inst.* 29: 1527–1535.
- [8] Bauwens CRL, Bergthorson JM, Dorofeev SB (2016) Experimental investigation of spherical-flame acceleration in lean hydrogen-air mixtures *Int. J. Hydrogen. Energy*. In Press.